Published in final edited form as:

Nature. ; 480(7376): 273–277. doi:10.1038/nature10557.

Aspartate[112] is the Selectivity Filter of the Human Voltage Gated Proton Channel

Boris Musset[1,†], **Susan M.E. Smith**[2,†], **Sindhu Rajan**[3], **Deri Morgan**[1], **Vladimir V. Cherny**[1], and **Thomas E. DeCoursey**[1,*]

[1]Department of Molecular Biophysics & Physiology, Rush University Medical Center, Chicago IL 60612 USA

[2]Department of Pathology, Emory School of Medicine, Atlanta GA 30322 USA

[3]Department of Medicine, University of Chicago, Chicago IL 60637 USA

Abstract

The ion selectivity of pumps and channels is central to their ability to perform a multitude of functions. Here we investigate the mechanism of the extraordinary selectivity of the human voltage gated proton channel[1], hH_V1. This selectivity is essential to its ability to regulate reactive oxygen species production by leukocytes[2–4], histamine secretion by basophils[5], sperm capacitation[6], and airway pH[7]. The most selective ion channel known, H_V1 shows no detectable permeability to other ions[1]. Opposing classes of selectivity mechanisms postulate that (a) a titratable amino acid residue in the permeation pathway imparts proton selectivity[1, 8–11], or (b) water molecules "frozen" in a narrow pore conduct protons while excluding other ions[12]. Here we identify Aspartate[112] as a crucial component of the selectivity filter of hH_V1. When a neutral amino acid replaced Asp[112], the mutant channel lost proton specificity and became anion selective or did not conduct. Only the glutamate mutant remained proton specific. Mutation of the nearby Asp[185] did not impair proton selectivity, suggesting that Asp[112] plays a unique role. Although histidine shuttles protons in other proteins, when histidine or lysine replaced Asp[112], the mutant channel was still anion permeable. Evidently, the proton specificity of hH_V1 requires an acidic group at the selectivity filter.

Voltage gated proton channels are considered specific (perfectly selective) for protons, because no evidence exists for permeation of anything but H^+. Specificity, combined with a

*Corresponding author: 1750 West Harrison, Chicago IL 60612 USA; phone: 312-942-3267; FAX: 312-942-8711, tdecours@rush.edu.
†These authors contributed equally to this work.

Supplementary Information accompanies the paper on www.nature.com/nature.

COMPETING FINANCIAL INTERESTS
The authors declare no competing financial interests.

AUTHORS' CONTRIBUTIONS
S.R. identified the similarity of C15orf27 to hH_V1 and cloned the C15orf27 gene; S.S. conceived the strategic approach based on molecular model, sequence, and phylogenetic analysis; S.R. and S.S. created mutants; T.D., B.M., and V.C. designed experiments; B.M., D.M. and V.C. recorded, analyzed, and interpreted data; T.D. wrote the manuscript; all authors read and approved the manuscript.

large deuterium isotope effect[9] and extraordinarily strong temperature dependence of conduction[10] suggests a permeation pathway more complex than a simple water wire, as exists in gramicidin[13]. All proton conduction appears consistent with a hydrogen-bonded chain (HBC) mechanism[14]; a HBC including a titratable group could explain several unique properties of H_V1[1], especially proton selectivity[14]. Yet in a recent study, mutation of each titratable amino acid in all four transmembrane (TM) helices of hH_V1 failed to abolish conduction[12]. Thus, the mechanism producing proton selectivity remained unknown.

We noticed that a human gene, C15orf27 (of unknown function), contains a predicted voltage sensor domain (VSD) that shares 25% sequence identity and 52% similarity [http://www.ebi.ac.uk/Tools/emboss/align/] with the VSD of hH_V1, and includes three Arg residues in the S4 TM helix that are conserved among all known H_V1 homologues. Phylogenetic analysis of VSD sequences (Fig. S1) reveals that a group comprising H_V1, C15orf27, and voltage sensitive phosphatase (VSP) sequences separated early from the two phylogenetically distinct groups of depolarization activated VSDs described previously (K_V channels and Na_V/Ca_V channels), supporting the modular evolution of VSD-containing proteins[15]. Furthermore, H_V1 VSDs occupy a discrete lineage, distinct from those of VSP and C15orf27 orthologs.

When we cloned the C15orf27 gene and expressed the product in HEK-293 or COS-7 cells, the GFP-tagged protein localised at the plasma membrane (Fig. S2), but we detected no currents beyond those in non-transfected cells. We reasoned that substitutions based on sequence elements that differ between hH_V1 and C15orf27 should be structurally tolerated while revealing residues responsible for proton conduction. We therefore mutated residues that are perfectly conserved in 21 H_V1 family members and differ between C15orf27 and H_V1. We replaced five candidate residues in hH_V1 (D112, D185, N214, G215, and S219) (Fig. 1a & 1b) with the corresponding residue in C15orf27. Four mutants exhibited large currents under whole-cell voltage clamp (Fig. 1d). The reversal (zero current) potential, V_{rev}, measured at several pH_o and pH_i, was close to the Nernst potential for protons, E_H (Fig. 1c), demonstrating proton selectivity. D112V mutants localised to the plasma membrane (Fig. S3), but displayed no convincing current (Fig. 1d). Some D112V transfected HEK-293 or COS-7 cells (and non-transfected cells) exhibited small native proton currents. His140A/H193A double mutants[16, 17], in which the two Zn^{2+} binding His residues are neutralized, resemble WT, with similar ΔpH dependent gating[12], and V_{rev} near E_H (Fig. S4). We expressed mutants in this Zn^{2+} insensitive background (D112x/A/A) to distinguish their currents from native currents that are abolished by 100 μM Zn^{2+} at pH_o 7.0. We tentatively concluded that Asp^{112} is crucial to proton conduction.

The absence of detectable currents in D112V led us to make other D112x substitutions. These mutants (Fig 2a) exhibited slowly activating outward currents upon depolarization that resembled hH_V1 currents. As reported previously[12], Asp^{112} mutation had little effect on the ΔpH dependence of gating. The proton conductance-voltage, g_H-V, relationship of all D112x mutants shifted roughly −60 mV when pH_o increased from 5.5 to 7.0 (Fig. S5), as in WT channels[1, 8, 18]. Mutation of Asp^{112} did influence channel opening and closing kinetics (Table S2).

Measurements of V_{rev} in Asp^{112} mutants revealed a marked departure from WT hH_V1 properties. At symmetrical pH 5.5, V_{rev} was near 0 mV (not shown). At pH_o 7.0, pH_i 5.5 (Fig. 2a, column 3), WT channels reversed near E_H (−87 mV), indicating proton selectivity. But for all mutants except D112E, V_{rev} was substantially positive to E_H (Fig. 2b), ranging from −58 mV (D112H) to −13 mV (D112N). Substitutions at Asp^{112} eliminated the proton specificity that distinguishes H_V1 from all other ion channels[1]. A previous study described currents in D112A and D112N mutants[12] but did not report V_{rev}.

We expected that loss of proton selectivity would result in nonselective permeation of cations. Surprisingly, V_{rev} did not change detectably when Na^+, K^+, N-methyl-D-glucamine$^+$, or TEA^+ replaced TMA^+ (Table S4). To test anion vs. cation selectivity, we adopted the classical tactic of replacing a fraction of the bath solution with isotonic sucrose[19]. The Nernst equation predicts that dilution of all extracellular ions except H^+ and OH^- (leaving internal ion concentrations unchanged) will shift V_{rev} negatively for a cation selective channel, but positively for an anion selective one. Despite the 10-fold reduction of buffer concentration, direct measurement confirmed that pH remained constant.

Fig. 3 illustrates determination of V_{rev} from tail currents in a D112H transfected cell at pH 5.5//5.5 in $CH_3SO_3^-$ (Fig. 3a) or Cl^- solution (Fig. 3c), and after 90% reduction of external ionic strength (Figs. 3b & 3d). Astonishingly, for all Asp^{112} mutants except D112K/A/A, sucrose shifted V_{rev} positively (Fig. S6), indicating anion selectivity both in $CH_3SO_3^-$ (Fig. 3e) and Cl^- solutions (Fig. 3f). For hH_V1 and D112E, V_{rev} did not change, reaffirming their proton specificity. Neutralization of a single Asp residue converts a proton channel into a predominantly anion selective channel. Thus, Asp^{112} mediates charge selectivity as well as proton selectivity.

To confirm anion permeability of Asp^{112} mutants, we replaced the main external anion, methanesulfonate$^-$ ($CH_3SO_3^-$), with Cl^-. Consistent with previous studies[1], V_{rev} in hH_V1 was unchanged. As shown in D112H (Fig. 3a vs. 3c), V_{rev} shifted negatively in Cl solutions in all mutants (except D112E), indicating that Cl^- is more permeant than the larger $CH_3SO_3^-$ anion (Fig. 3g). That all conducting non-acidic mutants exhibited Cl^-permeability indicates that Asp^{112} mediates not only proton selectivity, but also charge selectivity. Currents were smaller than WT in cells expressing some mutants (Fig. S7), suggesting a smaller unitary conductance. Evidently, these channels conduct anions, but not very well.

Although the mutant channels have diminished selectivity, V_{rev} did shift negatively when pH_o increased from 5.5 to 7.0 (Fig. 2b). Because these solutions differ mainly in buffer species and concentrations of H^+ and OH^-, Asp^{112} mutants must have significant permeability to H^+ and/or OH^-. The Goldman-Hodgkin-Katz equation shows how V_{rev} depends on ion concentrations:

$$V_{rev}=\frac{RT}{zF}\log\frac{P_{Cl^-}[Cl^-]_i+P_{CH_3SO_3^-}[CH_3SO_3^-]_i+P_{OH^-}[OH^-]_i+P_{H^+}[H^+]_o}{P_{Cl^-}[Cl^-]_o+P_{CH_3SO_3^-}[CH_3SO_3^-]_o+P_{OH^-}[OH^-]_o+P_{H^+}[H^+]_i}. \quad (1)$$

Ions with greater permeability dominate V_{rev}. Permeation of H^+ and OH^- are difficult to distinguish because they have the same Nernst potential[1]. The data can be interpreted assuming permeation of either (Table S3), but the anion selectivity of Asp^{112} mutants and the pH dependence of sucrose effects (Figs. 3e & 3f) support OH^- permeation. The relative permeability of conducting Asp^{112} mutants was OH^- (or H^+) > Cl^- > $CH_3SO_3^-$.

Although Asp^{112} is essential to selectivity, other acidic groups might participate. We mutated Asp^{185}, located in the presumed conduction pore (Fig. 1b)[12, 17]. However, like D185M (Fig. 1b), D185V, D185A, and D185N remained proton selective (Fig. S8). Speaking against additive effects, the double mutant, D112N/D185M did not differ from D112N (Fig. S8).

Consistent with earlier predictions that a titratable amino acid provides the selectivity filter of H_V1[1, 8–11], only channels with acidic residues (Glu or Asp) at position 112 manifested proton specificity. Asp^{112} lies at the constriction of the presumed pore (Fig. 1c), a logical location for a selectivity filter, and just external to the postulated gating charge transfer centre[20]. Our original prediction envisioned selectivity arising from protonation/deprotonation of a residue during conduction, but other mechanisms are possible. For example, proton selectivity of the influenza A M_2 viral proton channel has been explained by (a) immobilized water[21], (b) successive proton transfer and release by His^{37} (refs.[22, 23]), or (c) delocalization of the proton among His^{37} and nearby waters[24].

The Cl^- permeability of D112H was completely unexpected given strong precedents for His imparting proton selectivity to channels. Histidine shuttles protons in K^+ or Na^+ channel VSDs with Arg→His mutations[25–27], in carbonic anhydrase[28], and in M_2 channels[22, 23]. However, these molecules are not proton specific[27, 29]. Evidently, His shuttles protons, but does not guarantee proton selectivity. In hH_V1, Asp^{112} (or Glu^{112} in D112E) excludes anions, resulting in proton specific conduction. His may fail to exclude anions because it is cationic when protonated, whereas Glu and Asp are neutral.

The anion selectivity of neutral Asp^{112} mutants suggests that electrostatic forces due to the charge distribution in the rest of the channel deter cation permeation, and that the cation selectivity of the WT channel is due to the anionic charge of Asp^{112}. Asp^{185} does not participate directly in selectivity (Fig. S8). VSP family members possess the equivalent of Asp^{112} (Fig. 1a), yet conduct no current[30], illustrating that Asp^{112} requires a specific microenvironment to achieve selectivity. Although permeation of Cl^- and $CH_3SO_3^-$ suggests a wide pore in D112x mutants, local geometry might differ in WT channels due to the presence of anionic Asp^{112}.

Regulation of voltage gating by ΔpH is distinct from permeation. Pathognomonic of H_V1 is a strict correlation between the g_H-V relationship and V_{rev}, in which $V_{threshold}$ shifts 40 mV/Unit change in ΔpH[8]. The ΔpH dependence persisted in mutants exhibiting shifted g_H-V relationships [12]. Here we show uncoupling of V_{rev} and voltage gating. Asp^{112} mutants retained normal ΔpH dependence (Fig. S5), despite the dissociation of V_{rev} from ΔpH (Figs. 2 & S9). This uncoupling of pH control of gating from permeation speaks against any

mechanism that invokes regulation by local proton concentration in the vicinity of S4 Arg residues[12].

In summary, Asp^{112} is a critical component of the selectivity filter of hH_V1, crucial to both proton selectivity and charge selectivity. That D112E was proton selective, but D112H conducted anions indicates that this proton channel requires an acid at the selectivity filter. That neutralization of nearby Asp^{185} did not affect selectivity suggests that Asp^{112} plays a unique role.

'Methods Summary'

The pipette solution (also used externally) contained (mM) 130 $TMACH_3SO_3$, 2 $MgCl_2$, 2 EGTA, 80 MES, titrated to pH 5.5 with ~20 TMAOH. In the pH 5.5 TMACl solution, TMACl replaced $TMACH_3SO_3$. Bath solutions at pH 7.0 had (mM) 90 $TMACH_3SO_3$ or TMACl, 3 $CaCl_2$, 1 EGTA, 100 BES, and 36–40 TMAOH. For experiments with Zn^{2+}, solutions contained PIPES without EGTA. Experiments were done at 20–25°C. Currents are shown without leak correction. V_{rev} data were corrected for liquid junctions potentials measured in each solution[19].

'Methods'

Exhaustive searches to identify H_V1 homologs were performed using protein BLAST and PSI-BLAST. A sample of VSDs from K^+, Na^+, and Ca^{2+} channels (that open with depolarization like H_V1, and in addition one that opens with hyperpolarization), along with putative H_V1, VSP, and C15orf27 homologs were chosen. For cation channels, we sampled from the range of subfamilies, from the VSD repeats within Na^+ and Ca^{2+} channels, and from the range of species. VSD sequences, including crystallized K^+ channels (PDB ids 1ORS, 2R9R, and 2A79), were aligned using PromalS3D[31], which incorporates structural information, allowing high confidence identification of VSD boundaries. Sequences were trimmed to the VSD, realigned with PromalS3D, and the resulting alignment was analyzed with PhyML (maximum likelihood)[32] and Protpars (maximum parsimony)[33] at the Mobyle portal[34]. Trees were visualized with TreeDyn[35] and iTOL[36]. Parsimony (not shown) and maximum likelihood trees had similar topology, including H_V1 and C15orf27 families separating into discrete branches. A homology model of the VSD of hH_V1 was constructed as described previously[17].

The C15orf27 clone was PCR amplified from human cerebellum and subcloned into pcDNA3.1(+) expression vector (Invitrogen, Carlsbad, CA). The coding sequence of human H_V1 (*HVCN1*) was cloned into either pcDNA3.1(−) or pQBI25-fC3 (to make GFP-H_V1) vectors as described previously[16]. Site directed mutants were created using the Stratagene Quikchange (Agilent, Santa Clara, CA) procedure according to the manufacturer's instructions. All the positive clones were sequenced to confirm the presence of the introduced mutation. HEK-293 or, more often COS-7 cells were grown to ~80% confluency in 35 mm cultures dishes, usually by seeding cells 1 d ahead of transfection. Cells were transfected with 0.4–0.5 μg of the appropriate cDNA using Lipofectamine 2000 (Invitrogen). After 6 h at 37oC in 5% CO_2, the cells were trypsinized and re-plated onto glass cover slips at low density for patch clamp recording the following day. We selected

green cells under fluorescence for recording. Patch clamp methods were described previously[18].

The main pipette solution (also used externally) contained (in mM) 130 $TMACH_3SO_3$, 2 $MgCl_2$, 2 EGTA, 80 MES, titrated to pH 5.5 with ~20 TMAOH. In the pH 5.5 TMACl solution, TMACl replaced $TMACH_3SO_3$. Bath solutions at pH 7.0 had (mM) 90 $TMACH_3SO_3$ or TMACl, 3 $CaCl_2$, 1 EGTA, 100 BES, and 36–40 TMAOH. For experiments with Zn^{2+}, solutions contained PIPES buffer[37] without EGTA. Experiments were done at 20–25°C. Currents are shown without leak correction. V_{rev} data were corrected for liquid junctions potentials measured in each solution.

Supplementary Material

Refer to Web version on PubMed Central for supplementary material.

Acknowledgments

We thank Peter H. Barry, Dirk Gillespie, Vladislav S. Markin, John F. Nagle, Régis Pomés, David Silverman, and Valerij Sokolov for discussions or comments on the manuscript. Supported by NSF grant MCB-0943362 (SS & TD) and NIH grant GM087507 (TD). The content is solely the responsibility of the authors and does not necessarily represent the views of the National Institute of General Medical Sciences or the National Institutes of Health.

References

1. DeCoursey TE. Voltage-gated proton channels and other proton transfer pathways. Physiol Rev. 2003; 83:475–579. [PubMed: 12663866]
2. Capasso M, et al. HVCN1 modulates BCR signal strength via regulation of BCR-dependent generation of reactive oxygen species. Nat Immunol. 2010; 11:265–272. [PubMed: 20139987]
3. DeCoursey TE, Morgan D, Cherny VV. The voltage dependence of NADPH oxidase reveals why phagocytes need proton channels. Nature. 2003; 422:531–534. [PubMed: 12673252]
4. Henderson LM, Chappell JB, Jones OTG. The superoxide-generating NADPH oxidase of human neutrophils is electrogenic and associated with an H^+ channel. Biochem J. 1987; 246:325–329. [PubMed: 2825632]
5. Musset B, et al. A pH-stabilizing role of voltage-gated proton channels in IgE-mediated activation of human basophils. Proc Natl Acad Sci USA. 2008; 105:11020–11025. [PubMed: 18664579]
6. Lishko PV, Botchkina IL, Fedorenko A, Kirichok Y. Acid extrusion from human spermatozoa is mediated by flagellar voltage-gated proton channel. Cell. 2010; 140:327–337. [PubMed: 20144758]
7. Iovannisci D, Illek B, Fischer H. Function of the HVCN1 proton channel in airway epithelia and a naturally occurring mutation, M91T. J Gen Physiol. 2010; 136:35–46. [PubMed: 20548053]
8. Cherny VV, Markin VS, DeCoursey TE. The voltage-activated hydrogen ion conductance in rat alveolar epithelial cells is determined by the pH gradient. J Gen Physiol. 1995; 105:861–896. [PubMed: 7561747]
9. DeCoursey TE, Cherny VV. Deuterium isotope effects on permeation and gating of proton channels in rat alveolar epithelium. J Gen Physiol. 1997; 109:415–434. [PubMed: 9101402]
10. DeCoursey TE, Cherny VV. Temperature dependence of voltage-gated H^+ currents in human neutrophils, rat alveolar epithelial cells, and mammalian phagocytes. J Gen Physiol. 1998; 112:503–522. [PubMed: 9758867]
11. DeCoursey TE, Cherny VV. Voltage-activated hydrogen ion currents. J Membr Biol. 1994; 141:203–223. [PubMed: 7528804]
12. Ramsey IS, et al. An aqueous H^+ permeation pathway in the voltage-gated proton channel Hv1. Nat Struct Mol Biol. 2010; 17:869–875. [PubMed: 20543828]

13. Levitt DG, Elias SR, Hautman JM. Number of water molecules coupled to the transport of sodium, potassium and hydrogen ions via gramicidin, nonactin or valinomycin. Biochim Biophys Acta. 1978; 512:436–451. [PubMed: 81687]
14. Nagle JF, Morowitz HJ. Molecular mechanisms for proton transport in membranes. Proc Natl Acad Sci USA. 1978; 75:298–302. [PubMed: 272644]
15. Nelson RD, Kuan G, Saier MH Jr, Montal M. Modular assembly of voltage-gated channel proteins: a sequence analysis and phylogenetic study. J Mol Microbiol Biotechnol. 1999; 1:281–287. [PubMed: 10943557]
16. Ramsey IS, Moran MM, Chong JA, Clapham DE. A voltage-gated proton-selective channel lacking the pore domain. Nature. 2006; 440:1213–1216. [PubMed: 16554753]
17. Musset B, et al. Zinc inhibition of monomeric and dimeric proton channels suggests cooperative gating. J Physiol. 2010; 588:1435–1449. [PubMed: 20231140]
18. Musset B, et al. Detailed comparison of expressed and native voltage-gated proton channel currents. J Physiol. 2008; 586:2477–2486. [PubMed: 18356202]
19. Barry PH. The reliability of relative anion-cation permeabilities deduced from reversal (dilution) potential measurements in ion channel studies. Cell Biochem Biophys. 2006; 46:143–154. [PubMed: 17012755]
20. Tao X, Lee A, Limapichat W, Dougherty DA, MacKinnon R. A gating charge transfer center in voltage sensors. Science. 2010; 328:67–73. [PubMed: 20360102]
21. Sansom MSP, Kerr ID, Smith GR, Son HS. The influenza A virus M2 channel: a molecular modeling and simulation study. Virology. 1997; 233:163–173. [PubMed: 9201226]
22. Hu F, Luo W, Hong M. Mechanisms of proton conduction and gating in influenza M2 proton channels from solid-state NMR. Science. 2010; 330:505–508. [PubMed: 20966251]
23. Venkataraman P, Lamb RA, Pinto LH. Chemical rescue of histidine selectivity filter mutants of the M2 ion channel of influenza A virus. J Biol Chem. 2005; 280:21463–21472. [PubMed: 15784624]
24. Acharya R, et al. Structure and mechanism of proton transport through the transmembrane tetrameric M2 protein bundle of the influenza A virus. Proc Natl Acad Sci USA. 2010; 107:15075–15080. [PubMed: 20689043]
25. Starace DM, Bezanilla F. Histidine scanning mutagenesis of basic residues of the S4 segment of the shaker K^+ channel. J Gen Physiol. 2001; 117:469–490. [PubMed: 11331357]
26. Starace DM, Bezanilla F. A proton pore in a potassium channel voltage sensor reveals a focused electric field. Nature. 2004; 427:548–553. [PubMed: 14765197]
27. Sokolov S, Scheuer T, Catterall WA. Ion permeation and block of the gating pore in the voltage sensor of NaV1.4 channels with hypokalemic periodic paralysis mutations. J Gen Physiol. 2010; 136:225–236. [PubMed: 20660662]
28. Tu CK, Silverman DN, Forsman C, Jonsson BH, Lindskog S. Role of histidine 64 in the catalytic mechanism of human carbonic anhydrase II studied with a site-specific mutant. Biochemistry. 1989; 28:7913–7918. [PubMed: 2514797]
29. Leiding T, Wang J, Martinsson J, DeGrado WF, Årsköld SP. Proton and cation transport activity of the M2 proton channel from influenza A virus. Proc Natl Acad Sci USA. 2010; 107:15409–15414. [PubMed: 20713739]
30. Murata Y, Iwasaki H, Sasaki M, Inaba K, Okamura Y. Phosphoinositide phosphatase activity coupled to an intrinsic voltage sensor. Nature. 2005; 435:1239–1243. [PubMed: 15902207]
31. Pei J, Kim BH, Grishin NV. PROMALS3D: a tool for multiple protein sequence and structure alignments. Nucleic Acids Res. 2008; 36:2295–2300. [PubMed: 18287115]
32. Guindon S, Gascuel O. A simple, fast, and accurate algorithm to estimate large phylogenies by maximum likelihood. Syst Biol. 2003; 52:696–704. [PubMed: 14530136]
33. Felsenstein, J. Distributed by the author. Seattle: 1993.
34. Néron B, et al. Mobyle: a new full web bioinformatics framework. Bioinformatics. 2009; 25:3005–3011. [PubMed: 19689959]
35. Chevenet F, Brun C, Bauñls AL, Jacq B, Christen R. TreeDyn: towards dynamic graphics and annotations for analyses of trees. BMC Bioinformatics. 2006; 7:439. [PubMed: 17032440]

36. Letunic I, Bork P. Interactive Tree Of Life (iTOL): an online tool for phylogenetic tree display and annotation. Bioinformatics. 2007; 23:127–128. [PubMed: 17050570]

37. Cherny VV, DeCoursey TE. pH-dependent inhibition of voltage-gated H^+ currents in rat alveolar epithelial cells by Zn^{2+} and other divalent cations. J Gen Physiol. 1999; 114:819–838. [PubMed: 10578017]

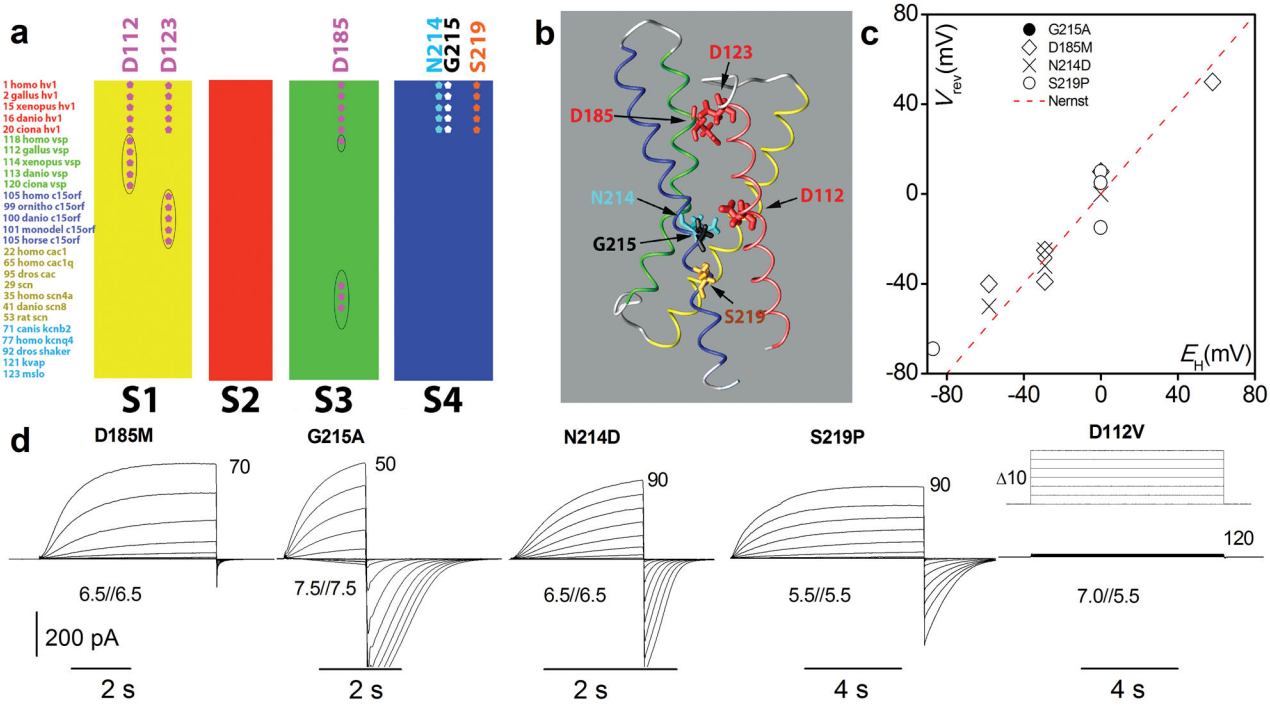

Figure 1. Identification of five key amino acids that differ in hH_V1 and C15orf27, and the currents generated in a heterologous expression system by hH_V1 mutants in which hH_V1 residues were replaced by the corresponding amino acid in the non-conducting C15orf27

a, Representative subset of multiple sequence alignment of 122 VSDs; only TM helices are shown. Gene families include: H_V1; voltage sensitive phosphatases; C15orf27; Ca^{2+} and Na^+ channels; and K^+ channels (cf. Fig. S1). **b**, Location of the key amino acids in the open hH_V1 channel VSD viewed from the side (membrane), based on a homology model[17]. **c**, V_{rev} in the four conducting mutants is near E_H (dashed line), indicating proton selectivity. V_{rev} was measured using tail currents; in G215A V_{rev} was positive to threshold and was observed directly. **d**, Voltage-clamp current families in cells expressing hH_V1 mutants. Depolarizing pulses were applied in 10-mV increments from a holding voltage, V_{hold} = −40 mV (D185M, D112V), −60 mV (G215A, S219P), or −90 mV (N214D), with the most positive pulse labelled. After membrane repolarisation, an inward "tail current" is seen as channels close (see inset for D185M); pH is given as $pH_o//pH_i$. D112V exhibited no clear current.

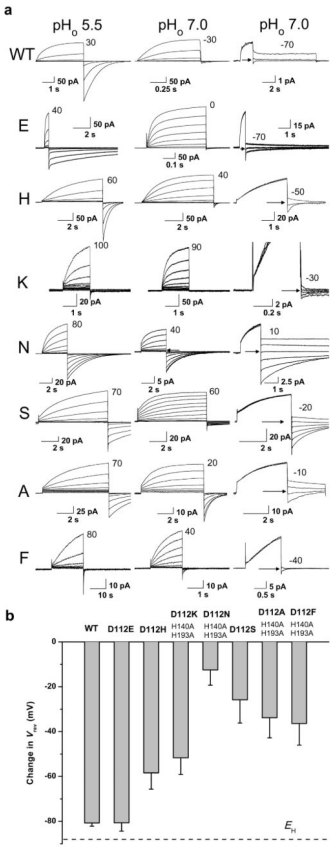

Figure 2. Currents in Asp112 mutants resemble proton currents, but are not

a, Currents generated by WT, D112E, D112H, D112K/A/A, D112N/A/A, D112S, D112A/A/A, and D112F/A/A in COS-7 cells (pH_i 5.5) at pH_o 5.5 (column 1) or 7.0 (column 2), during families of pulses in 10 mV increments up to indicated voltages. Tail currents at pH_o 7.0 (column 3) reveal that V_{rev} deviates from E_H, indicating loss of proton selectivity. At pH_o 5.5 V_{hold} was −40 mV (−60 mV for WT). At pH_o 7.0 V_{hold} was −40 mV (K, N, S), −50 mV (F), −60 mV (H, A), −80 mV (E), or −90 mV (WT); V_{pre} was −65 mV (WT), −40 mV (E), −10 mV (H), +50 mV (K), +40 mV (N, S), or +20 mV (A, F). V_{rev} (arrows) was determined from the amplitude and direction of tail current decay. For D112N, V_{rev} was above $V_{threshold}$ and was evident during pulse families. **b**, Shift in V_{rev} when the $TMACH_3SO_3$ bath solution was changed from pH 5.5 to 7.0. There is no difference between WT and D112E, but the shift in all other mutants is smaller than WT (p<0.001, by one-way ANOVA followed by Tukey's test, n = 7, 4, 9, 8, 6, 7, 9, and 4. Dashed line shows E_H.

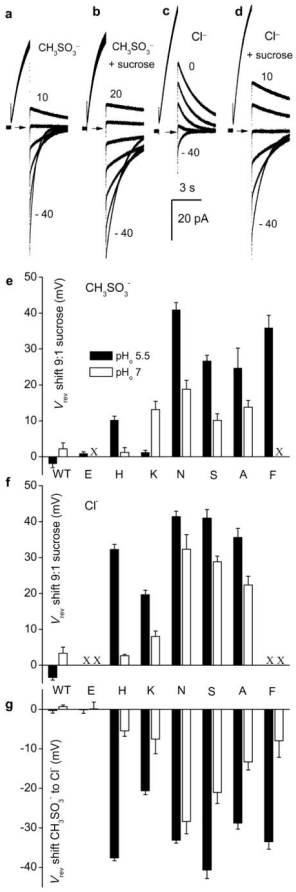

Figure 3. Dilution of ionic strength by 90% with isotonic sucrose shifted V_{rev} positively, indicating that most Asp^{112} mutants are anion selective

a Measurement of V_{rev} by tail currents in a cell transfected with D112H at pH 5.5//5.5 and (**b**) after sucrose. **c**, V_{rev} in the same cell in pH 5.5 Cl^- solution, and (**d**) after sucrose. Arrows indicate zero current. V_{hold} = −40 mV, V_{pre} = +60 mV. **e**, Mean shifts of V_{rev} with decreasing ionic strength in $CH_3SO_3^-$ solutions or (**f**) in Cl^- solutions. Each value was determined in 3–6 cells. X = not done. **g**, Shifts of V_{rev} when $CH_3SO_3^-$ was replaced by Cl^-. Values for WT and D112E do not differ significantly from 0 mV. For all anion selective mutants except D112N, the difference between shifts at pH 5.5 and 7.0 was significant (p<0.001, one-way ANOVA followed by Tukey's test; n = 3–8). Error bars in **e–g** are s.e.